PNAS
www.pnas.org

Supplementary Information for

Developmentally distinct CD4$^+$ T_{reg} lineages shape the CD8$^+$ T cell response to acute *Listeria* infection

Joseph S. Dolina, Joey Lee, Eugene L. Moore, Jennifer L. Hope, Donald T. Gracias, Takaji Matsutani, Ashu Chawla, Jason A. Greenbaum, Joel Linden, and Stephen P. Schoenberger*

***Correspondence:** Stephen P. Schoenberger

Email: sps@lji.org

This PDF file includes:

SI Materials and Methods

Animals

Male and female CD45.1$^+$ and CD45.2$^+$ C57BL/6, BALB/c, *Adora2a*$^{-/-}$ ($A_{2A}R$ deficient), CD45.1$^+$ and CD45.2$^+$ *Foxp3*^{eGFP} (FoxP3-eGFP), and *Foxp3*$^{DTR\text{-}eGFP}$ mice (The Jackson Laboratory, Bar Harbor, ME) were used in these experiments. *Foxp3*$^{DTR\text{-}eGFP}$ mice contain an internal ribosome entry site (IRES), human diphtheria toxin receptor (DTR), and an enhanced green fluorescent protein (eGFP) downstream of the internal stop codon of the *Foxp3* locus (1). In-house bred strains such as CD45.1$^+$ *Foxp3*^{eGFP} mice were generated from base strains obtained at The Jackson Laboratory and maintained for > 8 generations before usage. *Adora2a*$^{-/-}$ mice were backcrossed to BALB/c for 2 generations (using a speed congenic protocol) before arrival at The Jackson Laboratory and once thereafter to establish the colony. *Adora2a*$^{-/-}$ mice were compared to wild type C57BL/6 and BALB/c control mice purchased from The Jackson Laboratory in these experiments. Animals used were 8-12 weeks of age and maintained/bred in the La Jolla Institute for Immunology vivarium under specific pathogen-free conditions in accordance with guidelines of the Association for Assessment and Accreditation of Laboratory Animal Care International.

Infections

Listeria monocytogenes (*L. monocytogenes*) derived from the wild type 10403S background deficient in the actin assembly-inducing protein (Δ*actA*) and expressing amino acids spanning 138-338 of full-length ovalbumin (*L. monocytogenes* Δ*actA*-Ova) was obtained from the laboratory of Daniel A. Portnoy (University of California, Berkeley, CA). Bacteria were cultured in BBL brain heart infusion medium (Becton, Dickinson and Company, Sparks, MD) at 37°C, back-diluted to log-phase (OD_{600} = 0.075-0.100), washed, and re-suspended in 1×PBS. Primary in vivo infections were conducted via intravenous (IV) injection of 1×10^6 colony-forming units (CFU) *L. monocytogenes* Δ*actA*-Ova in the caudal vein.

In vivo antibody and small molecule treatments

Anti-CD73 (TY/23) and anti-TGF-β1/2/3 (1D11.16.8) (BioXCell, West Lebanon, NH) were used for in vivo blockade experiments. For early CD73 and TGF-β single or dual blockade, 250 μg of each antibody was delivered intraperitoneally (IP) every 24 h from day 0 to day 2, whereas late CD73 and TGF-β blockade regimens consisted of 250 μg antibody IP deliveries every 24 h from day 5 to day 6 relative to a day 0 infection. $CD25^{+}FoxP3^{+}CD4^{+}$ regulatory T cell (T_{reg}) depletion was achieved in *Foxp3*$^{DTR\text{-}eGFP}$ mice via IP administration of 100 μg/kg total diphtheria toxin (DT) from *Corynebacterium diphtheriae* (Sigma-Aldrich, St. Louis, MO) separated into quadruplicate 25 μg/kg IP injections at days −3, −1, 2, and 5 relative to a day 0 infection. Spleen mononuclear cells were harvested at day 7 for analysis of effects on the acute immune response.

In vitro antibody, peptide, and small molecule treatments

Blockade of suppression pathways during in vitro T cell suppressor assays was achieved by addition of 10 μg/mL total anti-Lag-3 (C9B7W), 20 μg/mL anti-TRAIL (N2B2) (BioLegend, San Diego, CA), 20 μg/mL anti-Gal-9 (RG9-1), 20 μg/mL anti-IL-10R (1B1.3A), 20 μg/mL anti-PD-L1 (10F.9G2) (BioXCell), or 10 μg/mL anti-TGF-β1/2/3 (1D11.16.8) (eBioscience, San Diego, CA). Interference in gap junction intercellular communication (GJIC) during culture occurred in the presence of 300 μM $Gap27_{204\text{-}214}$ connexin mimetic peptide and was compared to 300 μM scrambled control peptide (AnaSpec, Fremont, CA). For potent, selective inhibition of protein kinase A (PKA), 100 nM of KT5720 (Tocris/Bio-Techne Corporation, Minneapolis, MN) was included in select wells exposed to $Gap27_{204\text{-}214}$ or scrambled control peptides.

Survival surgery and hemisplenectomy

Separate collections of the dorso-cranial and ventral-caudal splenic lobes is possible in mice as the spleen is oxygenated by two arteries: the main ventral-dorsal artery branching from the arteria lienalis and the smaller dorso-cranial artery arising from the arteria mesenterica. To this end, mice

were shaved on the left flank at day 1 postinfection, and the area was cleaned with 5% povidone-iodine and 70% EtOH. Buprenex (buprenorphine; Reckitt Benckiser Pharmaceuticals, Slough, England, United Kingdom) was IP injected at 0.1 mg/kg 10 min prior to surgery. Under 2.5% isoflurane anesthesia, the abdominal cavity was entered via a transversal incision of the left flank. Colibri retractors were used to stabilize the opening. The spleen was gently luxated out of its anatomical position using organ-holding forceps, and the splenic vascular pole was dissected from the surrounding peritoneal adipose tissue with fine forceps. The dorso-cranial artery was clamped with a hemostat, ligated with 4-0 vicryl sutures, and cauterized proximal to the spleen. The spleen was then punctured with 4-0 vicryl sutures, and the dorso-cranial lobe was first secured by tying off the sutures followed by hemisplenectomy and collection of this portion. The open wound was cauterized, and the ventral-caudal splenic pole was placed back in its anatomical position. 1 mL of 0.9% sterile saline was delivered into the abdominal cavity to replenish fluid loss. The peritoneum and skin were closed with 4-0 vicryl sutures and staples, respectively. Animals were placed in a 37°C chamber and monitored until stable. Analgesic was administered 6-8 h after surgery and in the ensuing days if deemed appropriate. The ventral-caudal half of the spleen was terminally collected at day 7 postinfection. At both time points, untouched $CD4^+$ T cells were enriched using the EasySep Mouse $CD4^+$ T Cell Isolation kit (STEMCELL Technologies Inc., Vancouver, BC, Canada) and further subdivided into FoxP3-eGFP$^-$ conventional T cell (T_{conv}) and FoxP3-eGFP$^+$ T_{reg} fractions by fluorescence-activated cell sorting (FACS), described below. All sorted cells were re-suspended in 300 μL RNAprotect Cell Reagent (Qiagen, Valencia, CA) for TCR-Seq, described below.

Spleen mononuclear cell isolation

Spleens were excised from the abdominal cavities of naïve and infected mice and homogenized through sterile 70 μm cell strainers (Fisher Scientific, Pittsburgh, PA) in RPMI 1640 medium

containing 10% fetal bovine serum. Viable mononuclear cells were quantified via Trypan Blue exclusion on a Vi-CELL XR cell viability analyzer (Beckman Coulter, Indianapolis, IN).

In vitro T cell suppressor assays

Naïve CD45.1$^+$CD8$^+$ T responder cells (T_{resps}) were negatively sorted using the EasySep Mouse CD8$^+$ T Cell Isolation kit (STEMCELL Technologies Inc.) and stained with CellTrace Violet (CTV; Life Technologies, Carlsbad, CA). CD45.2$^+$CD4$^+$FoxP3-eGFP$^+$ T_{regs} from naïve *Foxp3*^{eGFP} mice or *L. monocytogenes* Δ*actA*-Ova infected *Foxp3*^{eGFP} mice at 1 or 7 d postinfection were enriched using the EasySep Mouse CD4$^+$ T Cell Isolation kit (STEMCELL Technologies Inc.) followed by FACS sorting of eGFP$^+$ cells. 5×10^4 CD45.1$^+$CD8$^+$ T_{resps} were placed in coculture with graded numbers of sex-matched, magnetic/fluorescent cell sorted CD45.2$^+$CD4$^+$FoxP3-eGFP$^+$ T_{regs} and 2 μL washed Mouse T-Activator anti-CD3/CD28 Dynabeads (Gibco, Carlsbad, CA) in a 96-well round-bottom plate for 72 h in RPMI 1640 medium containing 10% fetal bovine serum. For transwell experiments, T_{regs} and T_{resps} from the same mouse were seeded at a 1×10^5 cell density in upper and bottom chambers, respectively, of a Millicell 96-well flat-bottom plate containing a PCF membrane separation fenestrated with 0.4 μm pores (EMD Millipore, Billerica, MA). 2 μL washed Mouse T-Activator anti-CD3/CD28 Dynabeads were added to both chambers, and select wells contained 1 μM 5'-AMP (Sigma-Aldrich).

In a separate set of CD3/CD28-based suppressor assays, CD45.1$^+$CD4$^+$FoxP3-eGFP$^+$ T_{regs} were conversely used for assaying suppression of CD45.2$^+$CD8$^+$ T_{resps} of C57BL/6, BALB/c, and *Adora2a*$^{-/-}$ backgrounds in a 96-well round-bottom plate for a 72 h culture period. 1 μM 5'-AMP was included in select wells with cell contact unperturbed. Similar isolation procedures were used with these congenic and $A_{2A}R$ deficient strains.

Proliferation of CD8$^+$ T_{resps} in all experimental variations of T cell suppressor assays was determined by flow cytometry based on dilution of CTV. Percent suppression was calculated as

the percent difference in absolute number of dividing T_{resps} in wells containing $eGFP^+$ T_{regs} to the average absolute number of dividing T_{resps} in wells without addition of $eGFP^+$ T_{regs}.

Intracellular 3',5'-cyclic adenosine monophosphate (cAMP) assay

1.5×10^5 $CD4^+$FoxP3-$eGFP^+$ T_{regs} were isolated from naïve and infected *Foxp3*^{eGFP} mice as described above. Cells were re-suspended in a 40 µL mixture of 1×HBSS, 5 mM HEPES, 0.5 mM IBMX (Sigma-Aldrich), and 0.1% bovine serum albumin. Cells were lysed by adding 40 µL 0.6 M perchloric acid and 5.2 µL 0.36 M potassium carbonate to neutralize the acid. Lysed cells were placed on ice for 1 h, centrifuged at 10,000×g for 10 min at 4°C, and cAMP was quantified in the supernatant using the LANCE *Ultra* cAMP kit (PerkinElmer, Waltham, MA) according to the manufacturer's protocol. TR-FRET at 665 nm emission from a 340 nm excitation wavelength was measured using a SpectraMax M5 Microplate Reader equipped with SoftMax Pro (v7.0) software (Molecular Devices, San Jose, CA).

CD39/CD73 in vitro enzymatic assay and adenine nucleotide derivatization

$CD4^+$FoxP3-$eGFP^+$ T_{regs} and $CD4^+$FoxP3-$eGFP^-$ T_{convs} were isolated from naïve *Foxp3*^{eGFP} mice or those that had experienced *L. monocytogenes* Δ*actA*-Ova infection for 1 or 7 d as described above. Cells were rested for 2 h in serum-free RPMI 1640 medium and not vortexed upon transfer to new vessels in subsequent steps to avoid shearing of cells and release of cytoplasmic contents. 5×10^4 $eGFP^+$ T_{regs} or $eGFP^-$ T_{convs} were then placed in the upper chamber of a Millicell 96-well, 0.4 µm pore PCF membrane transwell plate (EMD Millipore). Cells were allowed to sink proximal to the membrane; the bottom chamber was pulsed 45 min later with either 10 µM 5'-AMP or 5'-ATP (Sigma-Aldrich) and gently mixed by pipette action. 15 min after pulsing, the bottom chamber was again gently mixed, and a cell-free 10 µL aliquot was collected and diluted 12× in 1 M acetate buffer (pH = 4.5) in a separate 96-well plate.

For conversion of adenine nucleotides contained in experimental samples or standards (diluted mixtures of Ado, 5'-AMP, 5'-ADP, and 5'-ATP) (Sigma-Aldrich) into fluorescent 1,N^6-etheno derivatives, a 50 µL aliquot of each sample or standard was mixed with 150 µL freshly prepared 7.87 M chloroacetaldehyde (Sigma-Aldrich):1 M acetate buffer (pH = 4.5) (11.2:138.8, v:v) in a glass 13-425 mm V-bottom Reacti-Vial (ThermoFisher Scientific, Waltham, MA). Mixtures were vortexed, centrifuged at 450×g for 2 min at 25°C, and then heated to 60°C for 60 min in a dry block heater with heated lid (VWR International, Radnor, PA) and a reservoir containing aluminum beads (Lab Armor, Cornelius, OR). When the derivatization reaction was complete, the vials were immediately placed at 4°C.

High-performance liquid chromatography (HPLC)

Shortly after derivatization and storage at 4°C, samples were loaded into a 96-well round-bottom plate and analyzed by reversed-phase HPLC. Separation of 1,N^6-etheno-adenine nucleotide derivatives was carried out as described previously (2) using a Prominence LC-20AT pump module equipped with an SIL-20A autosampler and in-line RF-20AXS fluorescence detector (Shimadzu Scientific Instruments, Columbia, MD). Pump control and peak integration was performed with LabSolutions software (v5.96 SP3) (Shimadzu Corporation, Tokyo, Japan). 1,N^6-etheno derivatives were detected using an excitation wavelength of 280 nm and emission wavelength of 410 nm. For each replicate of experiments, peak identification and calibration curves were generated using mixtures containing 0.5 to 40 pmol of each derivative. Except in cases where retention time drift resulted in an erroneous peak assignment from the peak table, identification and quantification of derivatives were automated using LabSolutions software post-run and browser modules. Peak integrations resulting in quantities below the lower limit of quantification (LLOQ) were assigned a value of 0.0.

Enzyme-linked immunosorbent assay (ELISA)

Cell culture supernatants were collected at day 3 in suppressor assays. The OptEIA Mouse IL-2 ELISA set (BD Biosciences, San Diego, CA) was used in this study according to the manufacturer's instructions. Absorbance was read at 450 nm using a SpectraMax M2 Microplate Reader equipped with SoftMax Pro (v5.3) software (Molecular Devices).

Fluorescence-activated cell sorting (FACS)

Cells were stained with the following fluorochrome-tagged monoclonal antibodies: anti-CD4 PE (GK1.5), anti-CD25 APC-R700 (PC61), anti-TNF PE-Cy7 (MP6-XT22) (BD Biosciences), anti-CD4 AF488 (RM4-5), anti-CD8α BV510 (53-6.7), anti-Gal-9 APC (RG9-35), anti-NK1.1 PerCP-Cy5.5 (PK136), anti-TGF-β1 (LAP) APC (TW7-16B4) (BioLegend), anti-pCREB (Ser133) PE (87G3) (Cell Signaling Technology, Danvers, MA), anti-CD4 APC-eF780 (RM4-5), anti-CD8α AF700, eF450 (53-6.7), anti-CD25 PE-Cy7 (PC61), anti-CD39 SB600 (24DMS1), anti-CD44 PerCP-Cy5.5 (IM7), anti-CD45.1 APC-eF780, eF450, PE (A20), anti-CD45.2 PE (104), anti-CD73 SB436 (eBioTY/11.B), anti-FasL APC (MFL3), anti-FoxP3 PE (FJK-16s), anti-IFN-γ APC (XMG1.2), anti-IL-10 APC (JES5-16E3), anti-Lag-3 APC (eBioC9B7W), anti-NK1.1 PE-Cy7 (PK136), anti-PD-L1 PerCP-eF710 (MIH5), anti-TCRβ APC-eF780 (H57-597), anti-TRAIL APC (N2B2) (eBioscience), anti-granzyme B (GrB) APC (GB11) (Invitrogen, Carlsbad, CA), anti-CD8α PE, PE-Cy7 (53-6.7), anti-CD25 PerCP-Cy5.5 (PC61), anti-CD45.2 APC (104), anti-CTLA-4 APC (UC10-4F10-11), anti-TCRβ APC, FITC (H57-597) (Tonbo Biosciences, San Diego, CA), and anti-A_{2A}R AF647 (7F6-G5-A2) (University of Virginia Antibody Engineering and Technology Core, Charlottesville, VA). Identification of cells in this study was achieved by an FSC-A versus SSC-A gate set at 30-250K versus 0-200K, respectively, including all leukocytes with the goal of excluding debris/reticulocytes/RBCs. Next, a singlet gate was set from 50-100K FSC-W parameter. An SSC-W singlet gate was not applied to avoid misconstruing blasting T cells as

doublets. In general, cell viability within this gate was > 97% using Live/Dead Fixable Yellow Dead Cell Stain kit (Invitrogen). For most experiments, live/dead stains were not deemed necessary unless mRNA was analyzed, which employed sorting out dead cells from analyzed populations. For T cells, a $TCR\beta^{+}NK1.1^{-}$ gate was applied to exclude $NK1.1^{hi}TCR\beta^{-}$ NK cells and $NK1.1^{lo}TCR\beta^{lo\text{-}hi}$ NKT cells. The resultant population contained 100% T cells, and further gates for CD4, CD8α, CD45.1, and CD45.2 were applied per the requirements of individual experiments. $CD4^{+}$ T cells were subsequently gated as T_{conv} ($FoxP3^{-}$) versus T_{reg} ($CD25^{+}FoxP3^{+}$). H-$2K^{b}$-Ova ($Ova_{257\text{-}264}$ bound to H-$2K^{b}$) iTAg tetramer (MBL International, Woburn, MA) was used to identify Ova-specific $CD8^{+}$ T cells. Any other analyte staining was based off fluorescence minus one (FMO) and isotype controls set at 0.5% positivity in negative control samples.

Cell surface staining of 3.0×10^{6} splenic mononuclear cells isolated directly ex vivo or various numbers of cells cultured in vitro was performed by specific antibody labeling for 15 min at 4°C in FACS Buffer (1×PBS containing 2% fetal bovine serum and 0.1% NaN_3). Cells were fixed in BD Cytofix/Cytoperm for 20 min at 4°C (BD Biosciences). GrB and CTLA-4 were assessed as direct ex vivo intracellular stains. Nuclear protein staining was achieved using the FoxP3 Staining set (eBioscience). For detection of phosphorylated proteins, cells were stained with the Transcription Factor Phospho Buffer set (BD Biosciences) according to the manufacturer's protocol. For intracellular and surface cytokine detection in T_{regs}, cells were restimulated with 5 ng/mL of phorbol 12-myristate 13-acetate (PMA) and 500 ng/mL of ionomycin (Sigma-Aldrich) for 5 h. For intracellular cytokine detection in antigen-specific $CD8^{+}$ T cells, cells were restimulated with 2 μg/mL $Ova_{257\text{-}264}$ (AnaSpec) for 5 h. Both cytokine procedures featured concurrent blocking with 1 μL/mL GolgiPlug and 1 μL/mL GolgiStop during culture and permeabilization with BD Perm/Wash (BD Biosciences) after fixation.

Assessment of cellular incorporation of 5-bromo-2'-deoxyuridine (BrdU) and 5-ethynyl-2'-deoxyuridine (EdU) was conducted by IP injecting *Foxp3*^{eGFP} mice with 1 mg EdU (Invitrogen)

at day 0 and 2 mg BrdU (BD Biosciences) at day 5 relative to day 0 *L. monocytogenes* Δ*actA*-Ova IV infections. $CD4^+$ T_{conv} and T_{reg} populations were first fluorescently sorted based off eGFP expression and then surface stained as described above to reach high T cell purity within the final gate. Cells were processed by combining the APC BrdU Flow kit (BD Biosciences) with the Click-iT EdU Pacific Blue Flow Cytometry Assay kit (Invitrogen) according to manufacturers' protocols as described previously (3).

Data were collected on BD FACS Canto II and Celesta flow cytometers (BD Immunocytometry Systems, San Jose, CA) and analyzed using FlowJo (v9.9.6) software (Tree Star Inc., Ashland, OR). t-Distributed Stochastic Neighbor Embedding (t-SNE) dimension reduction was performed using FlowJo (v10.5.3) software. t-SNE analysis of total $CD4^+$ T cell experimental replicates concatenated from 15,000-event downsampled files was performed using FoxP3, CD25, $A_{2A}R$, PD-L1, CD39, and CD73 markers not utilized for manually gating $CD4^+$ T cells ($NK1.1^-TCR\text{-}\beta^+CD4^+CD8^-$). t-SNE analysis of T_{regs} was similarly performed from 1,000-event downsampled files using $A_{2A}R$, PD-L1, CD39, and CD73 markers not utilized for manually gating the T_{reg} population ($NK1.1^-TCR\text{-}\beta^+CD4^+CD8^-CD25^+FoxP3^+$). FACS sorting of live pre-gated $NK1.1^-TCR\text{-}\beta^+CD4^+CD8^-$ cells followed by parsing of FoxP3-$eGFP^+$ and FoxP3-$eGFP^-$ populations was performed using BD FACSAria I, BD FACSAria II, and BD FACSAria Fusion cell sorters (BD Immunocytometry Systems). Pre-gating was not used for eGFP-based cell sorting during non-terminal in vitro assays to avoid potential effects of tethered antibodies; cells were rather pre-isolated using the EasySep Mouse $CD4^+$ T Cell Isolation kit (STEMCELL Technologies Inc.) prior to eGFP cell sorting as described previously.

TCR sequencing (TCR-Seq)

NGS-based TCR repertoire analysis was performed by Repertoire Genesis Inc. (Osaka, Japan). Total RNA was converted to cDNA with Superscript III reverse transcriptase (Invitrogen). A BSL-

18E primer containing polyT_{18} (Table S2) and a SphI site was used for cDNA synthesis. After cDNA synthesis, double strand (ds)-cDNA was synthesized with *Escherichia coli* (*E. coli*) DNA polymerase I (Invitrogen), *E. coli* DNA ligase (Invitrogen), and RNase H (Invitrogen). ds-cDNAs were blunted with T4 DNA polymerase (Invitrogen). A P10EA/P20EA adaptor (Table S2) was ligated to the 5' end of the ds-cDNA and then cut with SphI restriction enzyme. After removal of the adaptor and primer with MinElute Reaction Cleanup kit (Qiagen), PCR was performed with KAPA HiFi DNA polymerase (Kapa Biosystems, Woburn, MA) using either TCRα (*Tra*) chain constant region-specific (mCA1) or TCRβ (*Trb*) chain constant region-specific (mCB1) primers and P20EA (Table S2). PCR conditions were as follows: 98°C (20 sec), 65°C (30 sec), and 72°C (1 min) for 20× cycles. The second PCR was performed with either mCA2 or mCB2 and P20EA primers (Table S2) using the same PCR conditions. Amplicons were prepared by amplification of the second PCR products using P22EA-ST1-R and either mCA-ST1-R or mCB-ST1-R (Table S2).

After PCR amplification, index (barcode) sequences were added by amplification with Nextera XT Index kit v2 setA (Illumina, San Diego, CA). The indexed products were mixed in an equimolar concentration and quantified by a Qubit 2.0 Fluorometer (ThermoFisher Scientific). Sequencing was done with the MiSeq System (Illumina) using 300-bp paired-end reads (~1.0×10^5 *Tra* and ~1.8×10^5 *Trb* reads per condition). Assignment of sequences was performed by determining sequences with the highest identity in a data set of reference sequences from the international ImMunoGeneTics information system (IMGT) database (http://www.imgt.org). Data processing, assignment, and data aggregation were automatically performed using repertoire analysis software (RG software) originally developed by Repertoire Genesis Inc. RG software implemented a program for sequence homology searches using BLATN, an automatic aggregation program, and a graphics program for *Tra* and *Trb* V and J usage as well as CDR3 length distribution. Sequence identities at the nucleotide level between query and entry sequences were automatically calculated. Nucleotide sequences of CDR3 regions ranged from conserved cysteine

at position 104 (Cys104) of IMGT nomenclature to conserved phenylalanine at position 118 (Phe118), and the following glycine (Gly119) was translated to deduce amino acid sequences. Sequence reads having identical TRV, TRJ, and a deduced amino acid sequence of CDR3 was defined as a unique read. The copy number of unique reads were automatically counted by the RG software in each sample and then ranked in order of the copy number. Percentage occurrence frequencies of sequence reads with *Tra* V (TRAV), *Tra* J (TRAJ), *Trb* V (TRBV), and *Trb* J (TRBJ) genes in total sequence reads were calculated. Heatmaps of average *Tra* and *Trb* V and J gene segment family usage among infected animals were constructed using matrix2png (v1.2.1) (4). Shannon-Weaver TCR diversity indices were calculated using $H = -\sum_{i=1}^{S} p_i \, log_b \, p_i$ where p_i is the proportion of species i, and S is the number of species.

RNA sequencing (RNA-Seq)

Total RNA was purified using the Direct-zol RNA MiniPrep Plus and RNA Clean & Concentrator-25 kits (Zymo Research, Irvine, CA). RNA quality and quantity were assessed using an Agilent 2100 Bioanalyzer with an RNA 6000 Pico kit (Agilent Technologies, Santa Clara, CA) resulting in all samples producing RIN scores above 9.0. 5 ng of total RNA was then amplified using the Smart-seq2 protocol (5). A 1:1 ratio of Agencourt AMPure XP beads (Beckman Coulter) was used to purify resulting cDNA, and 1 ng cDNA was subsequently used to prepare a sequencing library with the Nextera XT DNA Library Prep kit (Illumina). Both whole-transcriptome amplification and sequencing library preparations were performed in a 96-well format to reduce assay-to-assay variability. Quality control steps were included to determine total RNA quality and quantity, the optimal number of PCR pre-amplification cycles, and fragment size selection. The resulting libraries were deep sequenced on the HiSeq 2500 System in Rapid Run mode (Illumina) using 50-bp single-end reads (~10.0×10^6 reads per condition).

Bioinformatics analysis of RNA-Seq

The single-end reads that passed Illumina filters were filtered for reads aligning to tRNA, rRNA, adapter sequences, and spike-in controls. Reads were then aligned to UCSC mm10 reference genome using TopHat (v1.4.1) software (6). DUST scores were calculated with PRINSEQ Lite (v0.20.3) software (7) and low-complexity reads (DUST > 4) were removed from the BAM files. Alignment results were parsed via the SAMtools (8) to generate SAM files. Read counts to each genomic feature were obtained with Python HTSeq (v0.7.1) software (9) using the 'union' option. After removing absent features (zero counts in all samples), raw counts were imported to R (v3.1.0) Bioconductor (v3.0) package DESeq2 (v1.6.3) (10) to score differentially expressed genes among samples. *P* values for differential expression were calculated using binomial test for differences between the base means of two conditions and then adjusted for multiple testing using the BH algorithm (11).

A row-scaled heatmap of log-transformed average reads per kilobase of transcript, per million mapped reads (RPKM) values was created with the 'heatmap.2' function in the gplots (v3.0.1) library under R (v3.3.3). Hierarchical clustering of samples was done with the 'hclust' function using average linkage. Gene set enrichment analysis (GSEA) (12) against the day 1 versus day 7 eGFP$^+$ T_{reg} comparison was performed with each of the 3 gene sets grouped by the hierarchical clustering above. Genes were pre-ranked by the $\log_{10}$ of their DESeq2 *P* value. Genes with a positive log fold change had their ranks multiplied by −1 before sorting and the 'classic' enrichment statistic was used. A volcano plot for the comparison of day 1 versus day 7 eGFP$^+$ T_{regs} was created with ggplot2 (v2.2.1) under R (v3.4.2). Shrunken $\log_2$ fold change (calculated via DESeq2) versus negative $\log_{10}$ *P* on the y-axis was plotted. A fold change cutoff of Δ1.5 was applied to color code differentially expressed genes. For principal component analysis (PCA), variance stabilizing transformation was applied on read counts for all samples. Data were generated in separate sequencing batches, and Combat (13) from the SVA package in R (v3.4.2) was used for

batch correction followed by PCA using prcomp in the stats library under R. The PCA plot was created with principal components 1 (PC1) and 2 (PC2) in x and y axes, respectively, using the ggplot function in ggplot2. Association of lymphocyte-related canonical pathways ($P < 0.05$ threshold for gene network overlap) with day 1 versus day 7 T_{regs} was conducted using Ingenuity Pathway Analysis (IPA; v01-07) software (Qiagen).

Statistical analysis

Significant differences between experimental groups were calculated using the two-tailed Student's t test, one-way ANOVA (with group comparisons ≥ 3), or linear regression where noted. Data analysis was performed using Prism (v7.0a and v8.0.2) software (GraphPad Software Inc., La Jolla, CA). Values of $P < 0.05$ were regarded as being statistically significant and noted as * < 0.05, ** < 0.01, *** < 0.001, and **** < 0.0001 (or denoted †). Each experiment in this report was replicated 2-4 times to ensure reproducibility and reach statistical power of the results.

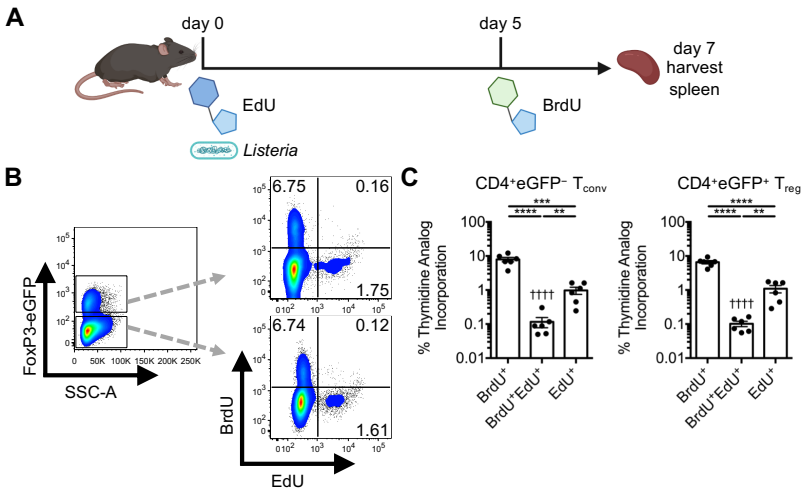

Fig. S1. Majority of day 1 versus day 7 CD4$^+$ T_{convs} and T_{regs} are developmentally unrelated. (A) *Foxp3*^{eGFP} mice infected with *L. monocytogenes* Δ*actA*-Ova concurrently given EdU IP during inoculation, followed by BrdU IP delivery at day 5. (B and C) FoxP3-eGFP$^-$ (T_{convs}) and FoxP3-eGFP$^+$ (T_{regs}) isolated at day 7 postinfection via magnetic/fluorescent sorting assessed for genomic incorporation of EdU and BrdU (n = 6 per group). Numbers in scatter plots represent percentage. Mean ± SEM; (C) $^{**}P < 0.01$, $^{***}P < 0.001$, and $^{****}P < 0.0001$ (Student's t test); $^{††††}P < 0.0001$ (one-way ANOVA).

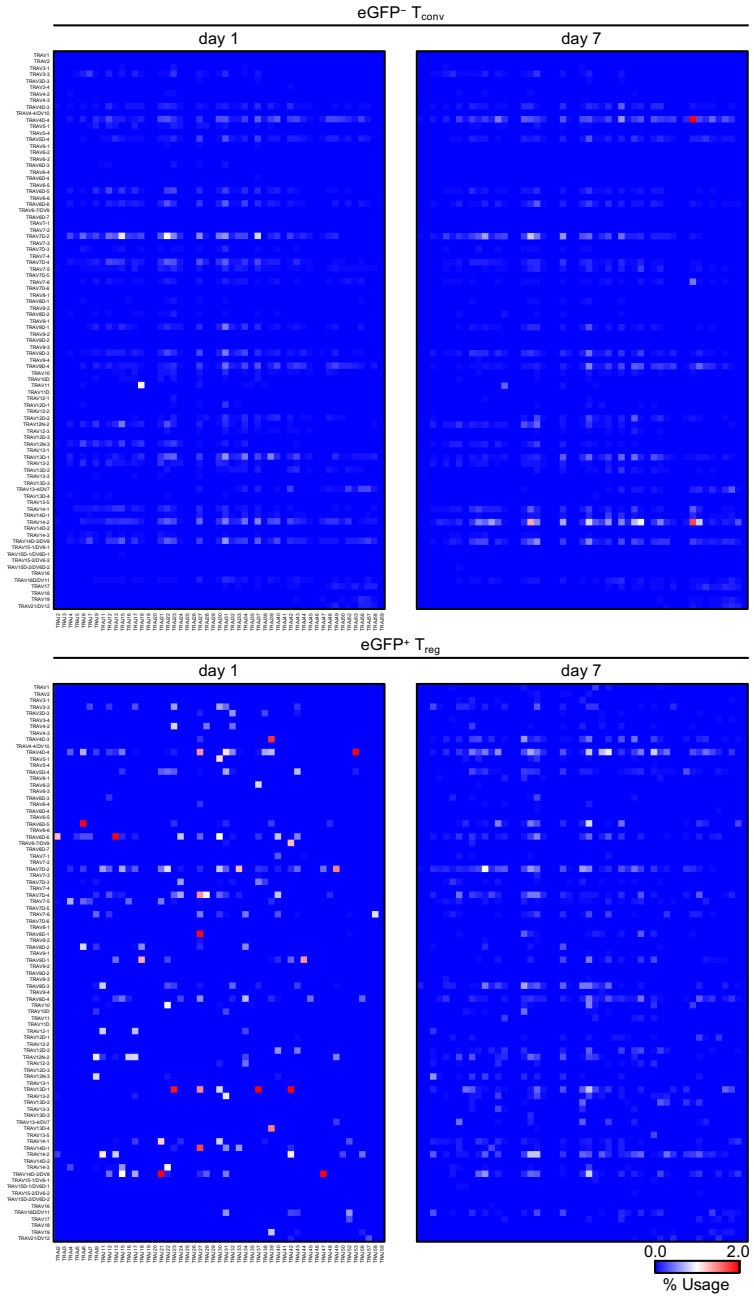

Fig. S2. *Tra* V, D, and J gene segment usage in T_{convs} and T_{regs} after *Listeria* infection. *Foxp3*^{eGFP} mice infected with *L. monocytogenes* Δ*actA*-Ova. Hemisplenectomy was performed at day 1 postinfection, and viable NK1.1^{-}CD4^{+}TCRβ^{+} FoxP3-eGFP^{-} (T_{conv}) and FoxP3-eGFP^{+} (T_{reg}) cell populations were cell sorted from the dorso-cranial lobe of the spleen. Corresponding cell populations were isolated at day 7 from the remaining ventral-caudal half of the spleen. Total RNA was isolated from all cells and subjected to TCR-Seq, with consideration of cell population comparisons originating from the same animal. Heatmaps showing TCRα *Tra* V (TRAV) and *Tra* J (TRAJ) gene segment family average usage among infected animals (n = 6 per group, 3 male and 3 female).

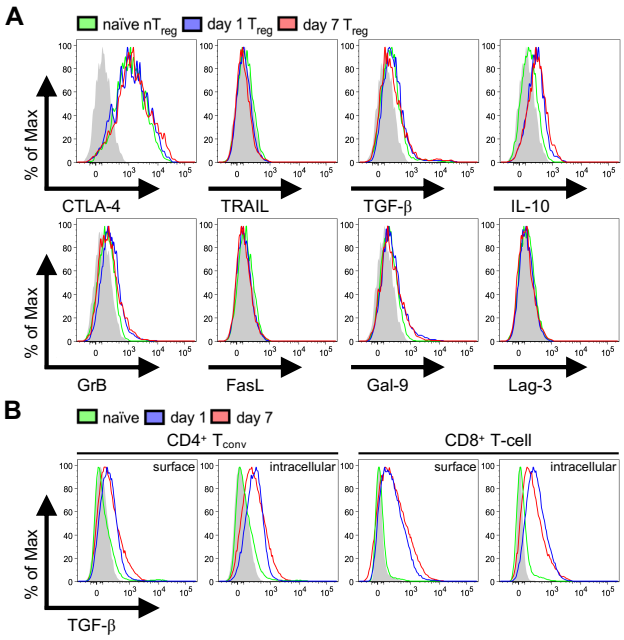

Fig. S3. Selected phenotypic profile of CD4$^+$ T$_{regs}$, CD4$^+$ T$_{convs}$, and CD8$^+$ T cells after *Listeria* infection. (A and B) C57BL/6 mice infected with *L. monocytogenes* Δ*actA*-Ova. (A) Expression of intracellular CTLA-4 and granzyme B (GrB) as well as surface TRAIL, TGF-β, FasL, Gal-9, and Lag-3 by CD25$^+$FoxP3$^+$CD4$^+$ T$_{regs}$ at various time points postinfection directly ex vivo. Intracellular IL-10 production by CD25$^+$FoxP3$^+$CD4$^+$ T$_{regs}$ restimulated with PMA and ionomycin (n = 4 per group). (B) Expression of surface displayed and intracellular TGF-β by FoxP3$^-$CD4$^+$ T$_{convs}$ and CD8$^+$ T cells from the same mice as in (A) at various time points postinfection separately restimulated with PMA and ionomycin (n = 4 per group).

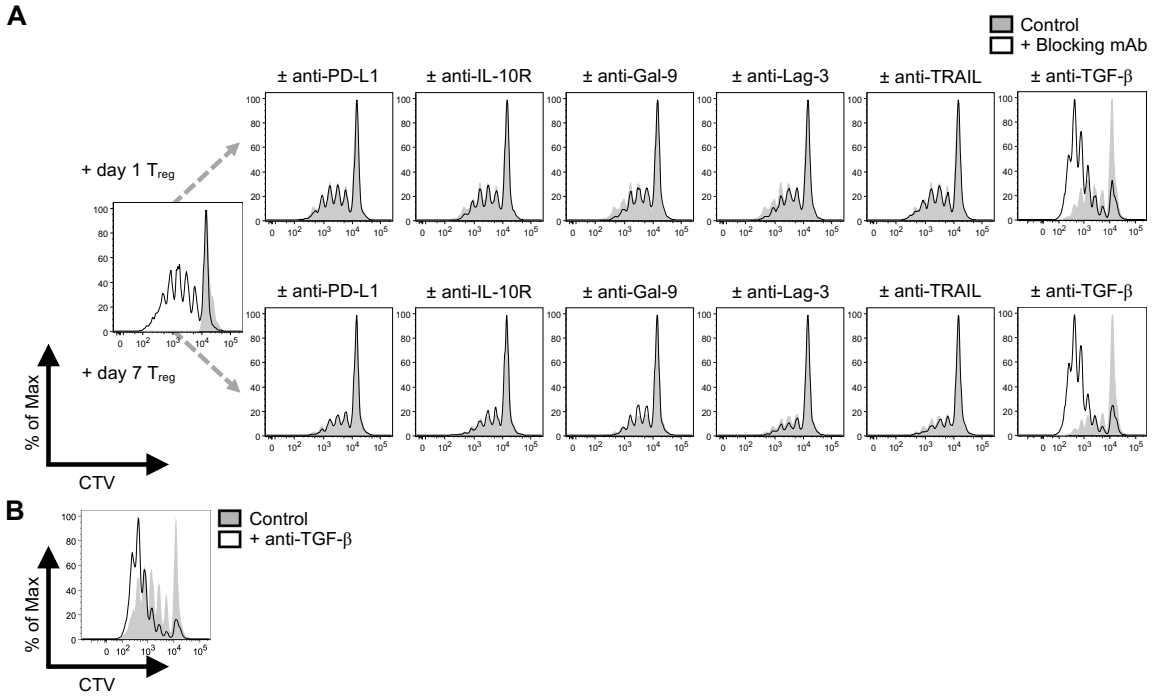

Fig. S4. Involvement of relevant pathways in T_{reg}-mediated suppression. (A) In vitro day 3 proliferation of naïve CTV-labeled $CD45.1^+CD8^+$ T_{resps} after coculture with $CD45.2^+CD4^+$FoxP3-$eGFP^+$ T_{regs} isolated from *Foxp3*^{eGFP} mice that underwent 1 or 7 d of *L. monocytogenes* Δ*actA*-Ova infection. Reported in histograms are data from 1:1 T_{reg}:T_{resp} cocultures with no additional treatment (control) versus cocultures containing blocking antibodies against PD-L1, IL-10R, Gal-9, Lag-3, TRAIL, and TGF-β (n = 4 per group). (B) $CD45.1^+CD8^+$ T_{resp} culture alone in the presence or absence of TGF-β antibody blockade without addition of T_{regs} (n = 4 per group).

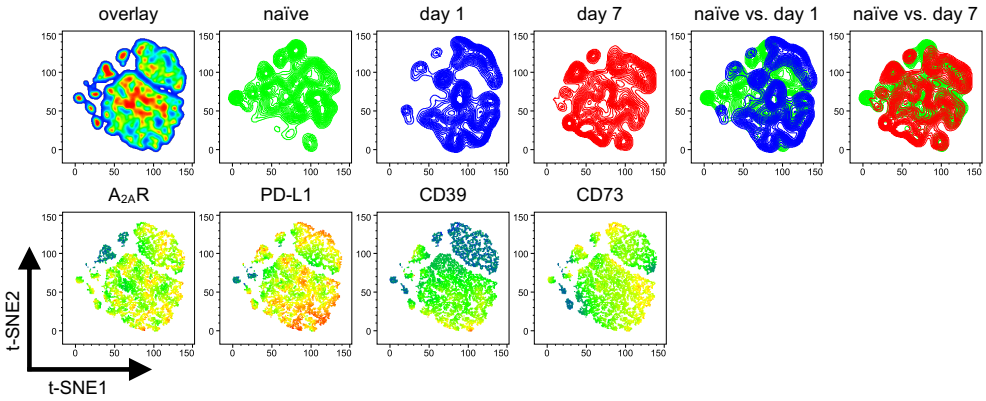

Fig. S5. Kinetic T_{reg} t-SNE comparison following *Listeria* infection. Naïve compared to day 1 and day 7 *L. monocytogenes* Δ*actA*-Ova infected C57BL/6 mice. t-SNE analysis on equal numbers of gated $CD25^{+}FoxP3^{+}CD4^{+}$ T_{regs} with $A_{2A}R$, PD-L1, CD39, and CD73 dimensions. Density plots (upper panel) and heatmap statistic displays of each input parameter (lower panel) displayed (n = 6 per group).

Table S1. Shared *Tra* and *Trb* reads in T_{conv} and T_{reg} populations.

TCRα eGFP$^-$ T_{conv}

Shared Reads #	Mean Reads ± SEM	TRAV	TRAJ	CDR3A
1	1171 ± 135	4D-4	48	CAAEANYGNEKITF
2	241 ± 111	14-2	40	CAASDTGNYKYVF
3	219 ± 145	14-2	39	CAASARNNAGAKLTF
4	194 ± 59	4D-4	48	CAAETNYGNEKITF
5	180 ± 79	4D-4	48	CAAEPNYGNEKITF
6	140 ± 87	14D-1	34	CAASPNTNKVVF
7	124 ± 59	14-2	16	CAASATSSGQKLVF
8	106 ± 92	14-2	22	CAAASSGSWQLIF
9	106 ± 90	14-2	48	CAASAGGNEKITF

TCRβ eGFP$^-$ T_{conv}

Shared Reads #	Mean Reads ± SEM	TRBV	TRBJ	CDR3B
1	554 ± 95	20	2-3	CGARDWGSAETLYF
2	370 ± 44	20	2-3	CGARDWGGAETLYF
3	237 ± 104	5	2-7	CASSQEGGSSYEQYF
4	199 ± 126	5	2-3	CASSPGLGPSAETLYF
5	192 ± 141	5	2-7	CASSQDYEQYF
6	192 ± 143	13-2	1-6	CASGDWNSPLYF
7	158 ± 156	5	2-7	CASSQEAGGSYEQYF
8	142 ± 71	20	2-3	CGARDWASAETLYF

TCRα eGFP$^+$ T_{reg}

Shared Reads #	Mean Reads ± SEM	TRAV	TRAJ	CDR3A
1	214 ± 103	12N-2	22	CALSASSGSWQLIF
2	211 ± 129	7D-2	15	CAASYQGGRALIF
3	81 ± 52	6D-6	34	CALGSSNTNKVVF
4	45 ± 14	7D-2	15	CAASTQGGRALIF
5	1 ± 0	12N-2	22	CALSTSSGSWQLIF

TCRβ eGFP$^+$ T_{reg}

Shared Reads #	Mean Reads ± SEM	TRBV	TRBJ	CDR3B
1	287 ± 137	13-2	2-7	CASGGTGGYEQYF
2	35 ± 24	14	2-3	CASSFSAETLYF
3	1 ± 0	13-1	2-5	CASTTAGGEDTQYF

Foxp3^{eGFP} mice infected with *L. monocytogenes* Δ*actA*-Ova. Hemisplenectomy was performed at day 1 postinfection, and viable NK1.1$^-$CD4$^+$TCRβ$^+$ FoxP3-eGFP$^-$ (T_{conv}) and FoxP3-eGFP$^+$ (T_{reg}) cell populations were cell sorted from the dorso-cranial lobe of the spleen. Corresponding cell populations were isolated at day 7 from the remaining ventral-caudal half of the spleen. Total RNA was isolated from all cells and subjected to TCR-Seq, with consideration of cell population comparisons originating from the same animal. Displayed are the top shared CDR3A and CDR3B reads with associated TCRα *Tra* V (TRAV) and *Tra* J (TRAJ) as well as TCRβ *Trb* V (TRBV) and *Trb* J (TRBJ) gene segment family usage, respectively, among T_{convs} and T_{regs} found in infected animals (n = 6 per group, 3 male and 3 female).

Table S2. TCR repertoire analysis primer list.

Primer	Sequence
BSL-18E	AAAGCGGCCGCATGCTTTTTTTTTTTTTTTTTTVN
P20EA	TAATACGACTCCGAATTCCC
P10EA	GGGAATTCGG
mCA1	TCATGTCCAGCACAGTTTTG
mCA2	GTTTTCGGCACATTGATTTG
mCB1	AGGATTGTGCCAGAAGGTAG
mCB2	TTGTAGGCCTGAGGGTCC
P22EA-ST1-R	GTCTCGTGGGCTCGGAGATGTGTATAAGAGACAGCTAATACGACTCCGAATTCCC
mCA-ST1-R	TCGTCGGCAGCGTCAGATGTGTATAAGAGACAGGTGGTACACAGCAGGTTCT
mCB-ST1-R	TCGTCGGCAGCGTCAGATGTGTATAAGAGACAGGTTGGGTGGAGTCACATTT

Listed are the various primers used during cDNA synthesis, adaptor ligation, and PCR preparation stages for application of TCR-Seq on NK1.1^{-}CD4^{+}TCRβ^{+} FoxP3-eGFP^{-} (T_{conv}) and FoxP3-eGFP^{+} (T_{reg}) cell populations sorted from hemisplenectomized mice.

SI References

1. Kim JM, Rasmussen JP, Rudensky AY (2007) Regulatory T cells prevent catastrophic autoimmunity throughout the lifespan of mice. *Nat Immunol* 8(2):191–197.

2. Bhatt DP, Chen X, Geiger JD, Rosenberger TA (2012) A sensitive HPLC-based method to quantify adenine nucleotides in primary astrocyte cell cultures. *Journal of Chromatography B* 889-890:110–115.

3. Gitlin AD, Shulman Z, Nussenzweig MC (2014) Clonal selection in the germinal centre by regulated proliferation and hypermutation. *Nature* 509(7502):637–640.

4. Pavlidis P, Noble WS (2003) Matrix2png: a utility for visualizing matrix data. *Bioinformatics* 19(2):295–296.

5. Picelli S, et al. (2014) Full-length RNA-seq from single cells usingSmart-seq2. *Nat Protoc* 9(1):171–181.

6. Trapnell C, Pachter L, Salzberg SL (2009) TopHat: discovering splice junctions with RNA-Seq. *Bioinformatics* 25(9):1105–1111.

7. Schmieder R, Edwards R (2011) Quality control and preprocessing of metagenomic datasets. *Bioinformatics* 27(6):863–864.

8. Li H, et al. (2009) The Sequence Alignment/Map format and SAMtools. *Bioinformatics* 25(16):2078–2079.

9. Anders S, Pyl PT, Huber W (2015) HTSeq--a Python framework to work with high-throughput sequencing data. *Bioinformatics* 31(2):166–169.

10. Love MI, Huber W, Anders S (2014) Moderated estimation of fold change and dispersion for RNA-seq data with DESeq2. *Genome Biol* 15(12):550.

11. Benjamini Y, Hochberg Y (1995) Controlling the False Discovery Rate: A Practical and Powerful Approach to Multiple Testing. *Journal of the Royal Statistical Society* 57(1):289–300.

12. Subramanian A, et al. (2005) Gene set enrichment analysis: a knowledge-based approach for interpreting genome-wide expression profiles. *Proc Natl Acad Sci USA* 102(43):15545–15550.

13. Johnson WE, Li C, Rabinovic A (2007) Adjusting batch effects in microarray expression data using empirical Bayes methods. *Biostatistics* 8(1):118–127.